Rend. Fis. Acc. Lincei (2015) 26:263–270
DOI 10.1007/s12210-015-0417-2

Decoration of magnesium oxide nanoparticles on O-MWCNTs and its antibacterial studies

Y. T. Prabhu[1] · K. Venkateswara Rao[1] · B. Siva Kumari[2] · Tambur Pavani[1]

Received: 16 January 2015 / Accepted: 28 March 2015 / Published online: 17 April 2015

Abstract Magnesium oxide nanoparticles in their pure phase are carefully and homogenously decorated by a facile approach on oxygen-functionalized multi-walled carbon nanotubes (O-MWCNTs) using magnesium nitrate. Magnesium oxide nanocrystals imbued on O-MWCNTs were examined for its structure and morphology by various techniques, such as powder X-ray diffraction, Fourier transform infrared spectroscopy, transmission electron microscopy and field emission scanning electron microscopy. The nanocrystals on the O-MWCNTs were determined to be 20–25 nm size. Magnesium oxide nanocrystal's dislocation density and microstrain are calculated. Thermogravimetric measurements are studied for the weight loss. The antibacterial studies are performed against a set of bacterial strains. It has shown its antibacterial properties on both gram-positive and gram-negative bacterial strains.

Keywords Multi-walled carbon nanotubes (MWCNTs) · X-ray diffraction (XRD) · Magnesium matrix composites · TEM · Thermal analysis · Zeta potential · Antibacterial activity

✉ Y. T. Prabhu
ytprabhusj@gmail.com

[1] Center for Nano Science and Technology, Institute of Science and Technology, Jawaharlal Nehru Technological University Hyderabad, Hyderabad 500085, India

[2] Botany Department, Andhra Loyola College, Vijayawada, Andhra Pradesh, India

1 Introduction

From the time of the discovery of nanotubes which have been widely used due to their atomic structure, they have good mechanical, electrical and thermal properties. Multi-walled carbon nanotubes (MWCNTs) have also gained attention in the biomedical, aerospace, biosensor and electronics application (Khare and Bose 2005; Park et al. 2002). In our modern times, studies on polymer nanocomposites are widely done due their numerous applications in many different industrial sectors. In the area of nanostructured hybrid materials, specifically bio-nanocomposites are showing bright results. Natural polymers combine with organic or inorganic solids forming bio-nanocomposites and also at the nanometer scale. We know that most of the synthetic polymers are not biocompatible so the use of bio-nanocomposites has been preferred. There are earlier studies revealing that chitosan (CTS) and carbon nanotubes (CNT) form a very attractive bio-nanocomposite which were used for biosensor modification (Park et al. 2002; Erdema et al. 2012; Pauliukaite et al. 2010), preparation, structural characterization and mechanical properties (Carson et al. 2009; Wang et al. 2005; Shieh and Yang 2006; Hao et al. 2007; Ke et al. 2007; Liu et al. 2009; Tang et al. 2009).

The complex nature of the composite is very difficult to explain the complete internal structural details of the conducting medium in the polymer nanocomposites. The microscopic and macroscopic states of the composites govern the electrical conductivity. The information inside the composite material systems is understood by the interaction of the individual components. One of the most appropriate and sensitive approaches for understanding polymer structures is defining the electrical properties and zeta potential of a material (Basavaraja et al. 2010).

For the antibacterial activity, several polymer-based composites were investigated. There were many positive results of antibacterial polymers with inherent antibacterial properties (Campoccia et al. 2013). The decoration of metal nanoparticles on carbon nanotubes showed a potential application as a new hybrid material in the study of antibacterial activity, gas sensors and electrical conductivity enhancement (Shameli et al. 2012; Shameli 2013). It was reported in the earlier studies that it was difficult to decorate metal and metal oxides on the surface of the MWCNTs (Sahoo et al. 2011). The nanoparticles could be attached to MWCNTs only if a strong interaction force is induced between MWCNTs and nanoparticles. Thus, chemical functionalization is needed. The strong acids such as HNO_3 and H_2SO_4 are used for the formation of hydroxyl and carboxylic groups on the surfaces of MWCNTs. Nucleation of the metal and metal oxides takes place by this technique (Xu et al. 2004). We are particularly interested in metal oxides such as ZnO, MgO, TiO_2 and CaO as they are not only stable but also considered as safe material to human beings and animals (Stoimenov et al. 2002). Recently studies were made on MgO showing the high influence against bacteria. There are also results that there is high potent in toxic waste remediation (Sawai et al. 2000; Sawai 2003; Makhluf et al. 2005; Tiwari et al. 2008; Nagappa and Chandrappa 2007).

In the present paper, we have shown an easy way to decorate magnesium oxide nanoparticles on O-MWCNTs. We have studied the antibacterial activity against gram-negative bacteria (*Escherichia coli*) and gram-positive bacteria (*Staphylococcus aureus*). This study could give clue that such materials are capable of antibacterial activity and also could be useful in the study of water purification and medical purpose.

2 Experimental details

2.1 Functionalized of MWCNTs

The functionalized MWCNTs are formed by treating MWCNTs with mixture of concentrated H_2SO_4 and HNO_3 with the molar ratio of 3:1 (DeJesus et al. 2005; Lin et al. 2010). 75 ml of H_2SO_4 (97 %) and 25 ml of conc. HNO_3 (65 %) are carefully mixed together to this mixture; 1 g of MWCNTs is added in a round-bottom flask which is subjected to heating at 50 °C under constant stirring for 8 h. Now it is allowed to cool to room temperature, further add same amount of deionized water and filter the solution. Wash the residue 3–4 times with distilled water. In order to obtain neutral pH, add deionized water. The residue is dried, and thus oxygen-functionalized MWCNTs are obtained.

2.2 Decoration of magnesium nitrate on O-MWCNT

One hundred milligrams of O-MWCNTs is taken in 70 ml of isopropyl alcohol (IPA) and ultrasonicated till good suspension and dispersion are obtained. Magnesium nitrate $[Mg(NO_3)_2{\cdot}6H_2O]$ is taken as precursor for the decoration of magnesium oxide. 77.2 mg of magnesium nitrate (15 wt% of Mg) is suspended in 30 ml of isopropyl alcohol (IPA) for 2 h. After an hour of aging, a viscous solution is formed. Both the solutions are mixed and kept under stirring for 4 h. The whole solution is allowed to cool to room temperature. It is filtered and washed with acetone. At 300 °C the sample is annealed in the furnace for 1 h. It is dried at room temperature.

2.3 Antibacterial activity studies

The well-diffusion technique (Chung et al. 1998) is employed where bacterial strains (*Staphylococcus aureus* and *Escherichia coli*) are used in our tests. These bacterial strains are taken from the stock collection from Centre of Biotechnology, Institute of Science and Technology, Jawaharlal Nehru Technological University Hyderabad,

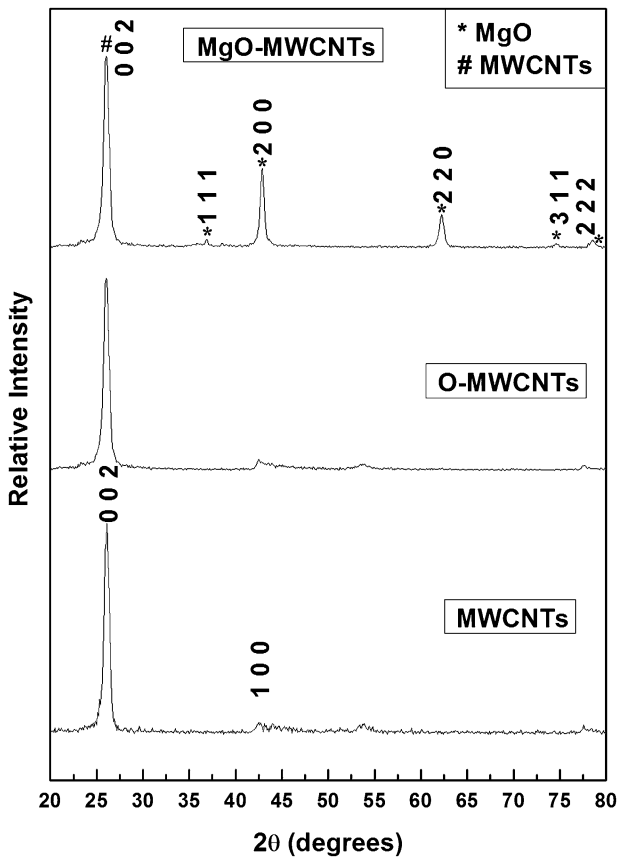

Fig. 1 XRD patterns of MWCNTs, O-MWCNTs, MgO-MWCNTs

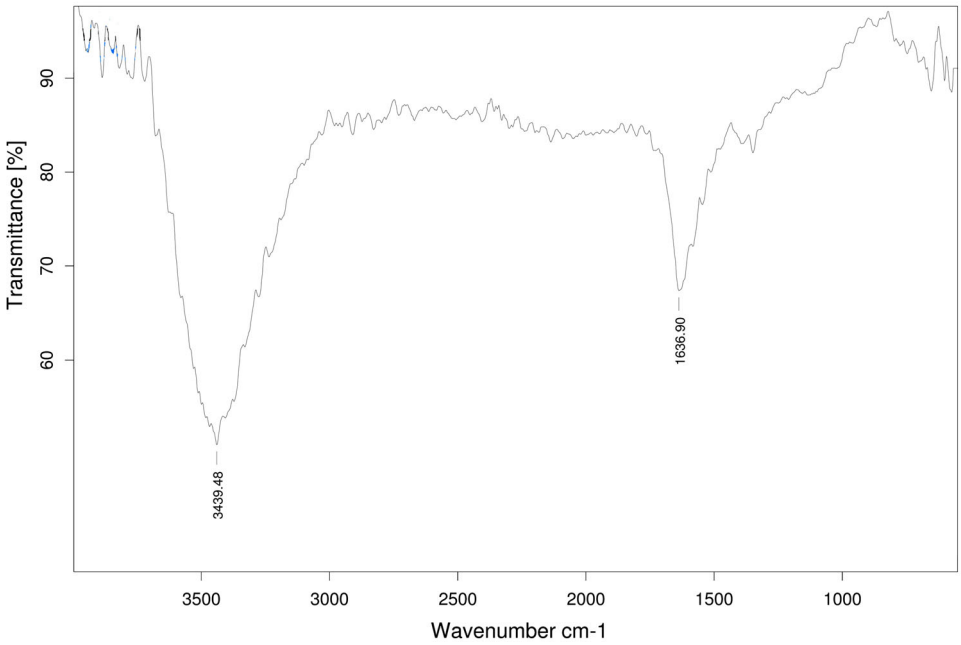

Fig. 2 FT-IR spectra of O-MWCNTs

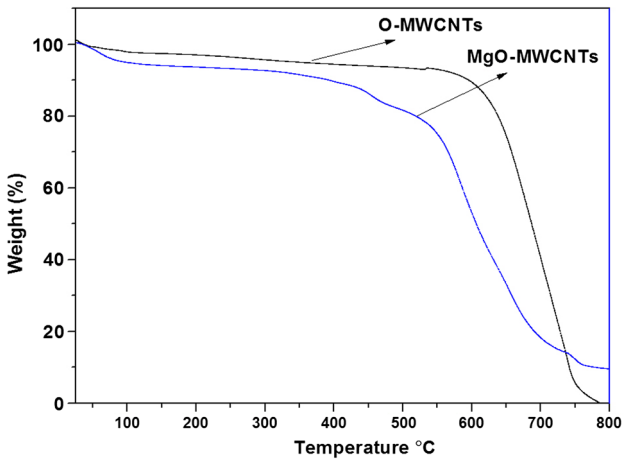

Fig. 3 TGA curves of O-MWCNTs, MgO-MWCNTs

Hyderabad. Five hundred microliters of nutrient broth culture of each bacterial organism is added to 100 ml solution of different concentration of MgO-MWCNTs ranging from 50 to 200 µg/ml. With parafilm tape, the plates are wrapped and are transferred to incubator which is maintained at 37 °C for 24 h. The inhibition zones are recorded in centimeters.

3 Results and discussion

3.1 XRD

The X-ray diffraction pattern is obtained by using copper radiation with X-ray wavelength of 1.54 Å. In Fig. 1 XRD pattern of MWCNTs, O-MWCNTs and MgO-MWCNTs is shown. The two diffraction peaks at $2\theta = 26°$ and 43° correspond to *hkl* reflections (002) and (100), respectively, for O-MWCNTs indicating that MWCNTs are unbroken even after the acid treatment (Liu et al. 2006). MgO nanocrystals have five distinct peaks at 37°, 43°, 62°, 74° and 78° corresponding to (111), (200), (220), (311) and (222) *hkl* planes on the surface MgO-MWCNTs (Kondoh et al. 2010). The XRD data obtained are in good agreement with the JCPDS #75-1525 corresponding to the face centered cubic structure of magnesium oxide. The lattice constants of MgO nanoparticles are a = b = c = 4.198 Å. There are no other peaks other than MgO indicating the purity of the composite formation. By using the Debye–Scherrer equation, the crystalline size of the composite is calculated (Pal and Chauhan 2009). The crystallite size of nanoparticles on O-MWCNTs is 25 nm.

$$D = \frac{0.9\lambda}{\beta \cos\theta} \tag{1}$$

where λ, β and θ are the X-ray wavelength, full width at half maximum (FWHM) of the diffraction peak and Bragg's diffraction angle, respectively. Dislocation density (δ) is calculated from the crystalline size. The cumulative dislocation density is 1.65×10^{16} Lines/m^2.

$$\delta = \frac{1}{D^2} \tag{2}$$

Microstrain arises due to the lattice misfit, which varies on the deposition conditions calculated by the formula. The collective microstrain is 1.72×10^{-3} Lines^{-2}/m^4.

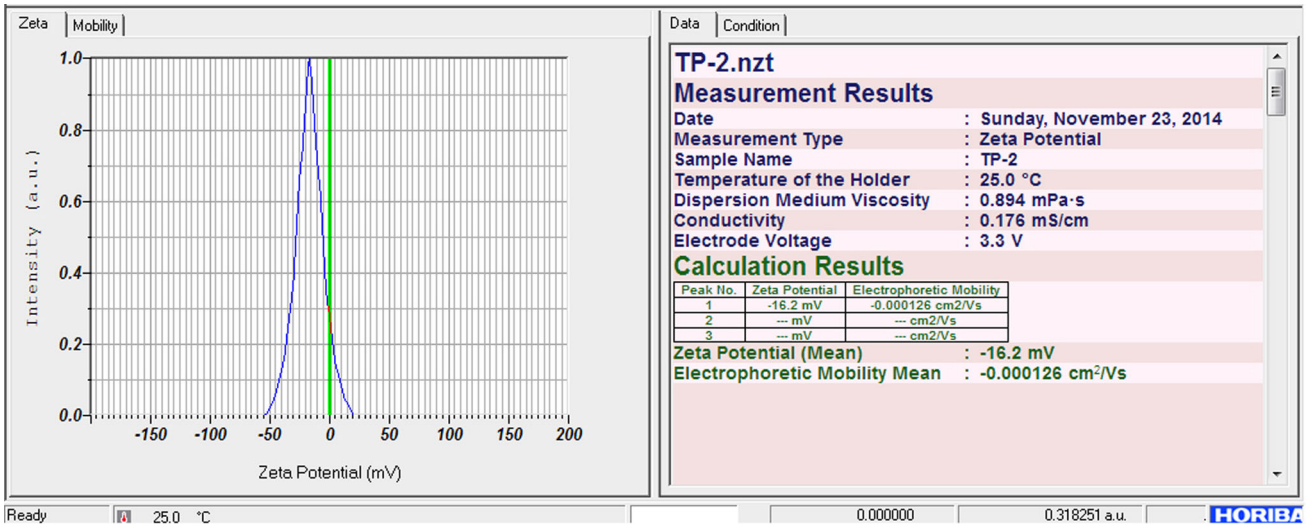

Fig. 4 Zeta potential of MWCNTs

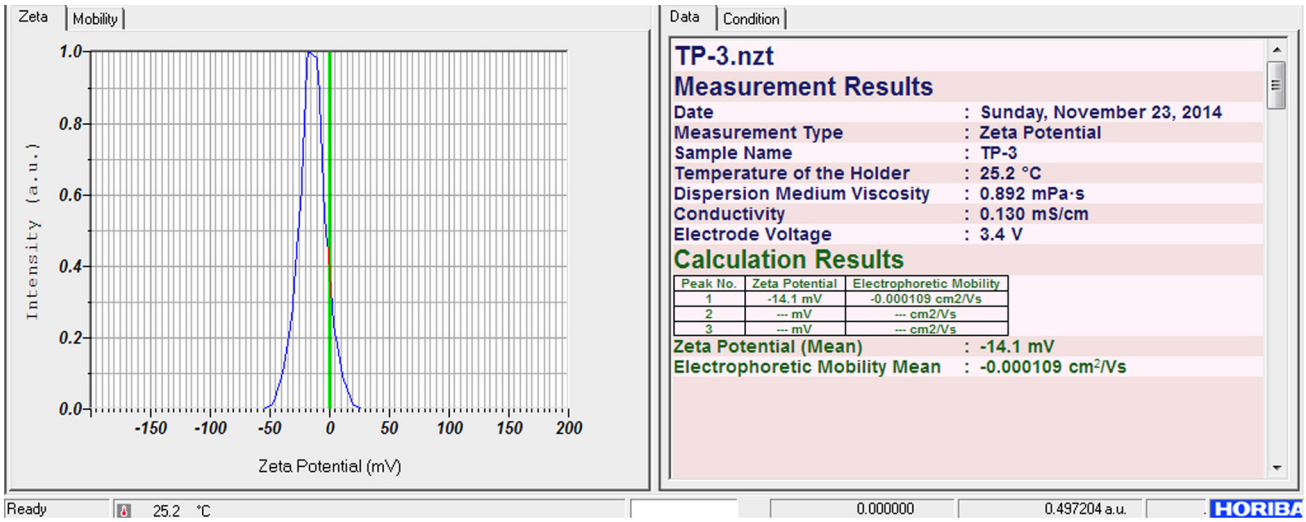

Fig. 5 Zeta potential of O-MWCNTs

$$\varepsilon = \frac{(\beta \cos \theta)}{4}. \quad (3)$$

3.2 Fourier transform infrared spectroscopy (FT-IR) analysis

The active sites of O-MWCNTs assist in anchoring magnesium oxide nanoparticles on it. O-MWCNTs are investigated by FT-IR which is shown in Fig. 2. O–H stretching frequency is originating by the absorption of water molecules on the amorphous carbon in the CNTs (Titus et al. 2006) which can be ascribed to the peak around 3439 cm^{-1}. C=C stretching frequency is assigned to the two peaks 1636 cm^{-1}.

3.3 TGA

The moisture content, the weight ratio of the O-MWCNTs and grafted organic material (MgO) on MgO-MWCNTs are calculated from the thermogravimetric measurements. They are shown in Fig. 3. The weight of O-MWCNTs remained 90.65 % at 800 °C, and the 9.35 % weight loss could have come from the disintegration of OH groups and COOH groups. The weight of MgO-MWCNTs remained 80.20 % at 800 °C, and the 19.8 % weight loss could be

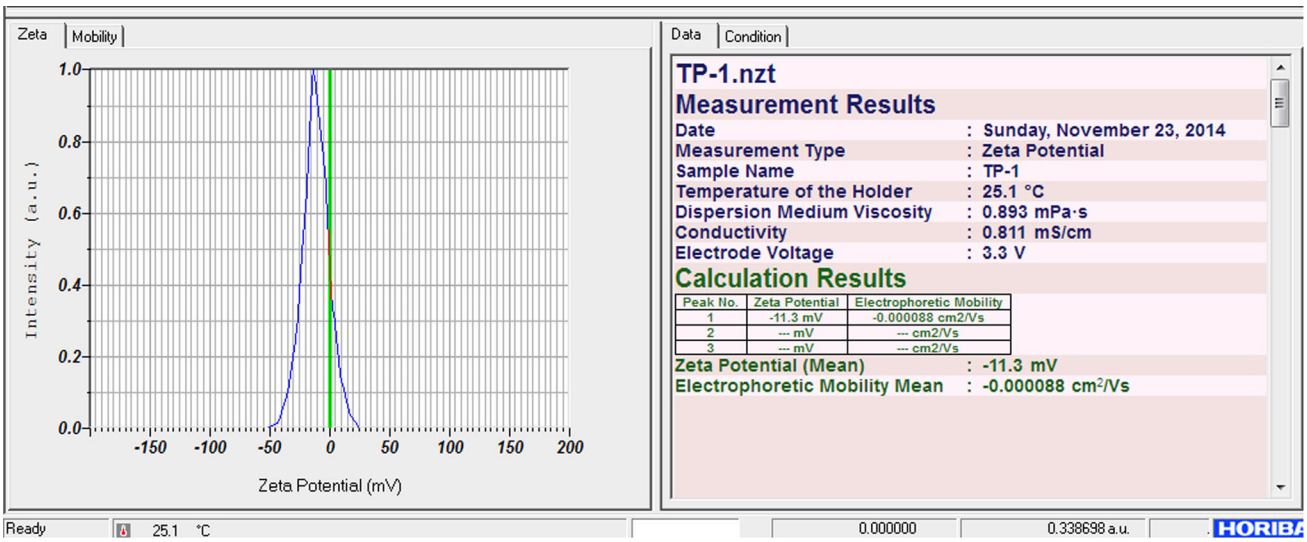

Fig. 6 Zeta potential of MgO-MWCNTs

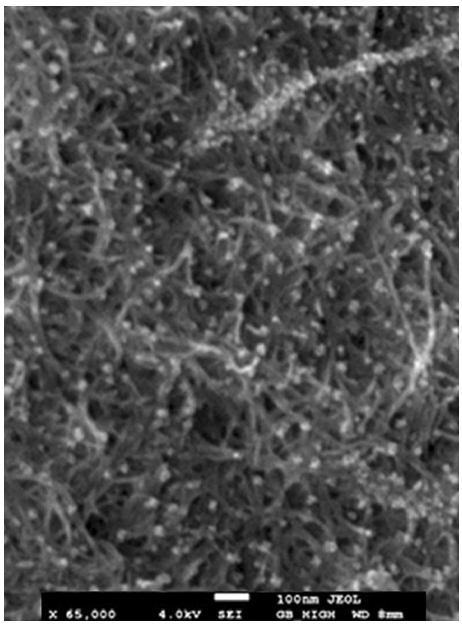

Fig. 7 FE-SEM micrograph of MgO-MWCNTs

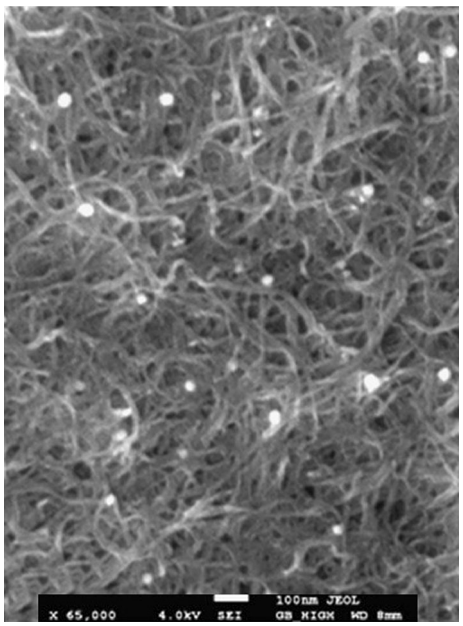

Fig. 8 FE-SEM image of MgO-MWCNTs

due to loss of metal oxide and disintegration of other OH groups and COOH groups.

3.4 Zeta potential

MWCNTs, O-MWCNTs and MgO-MWCNTs samples are dispersed in ethanol and are subjected to zeta potential test in the instrument HORIBA SZ-100 particle size analyzer. Their results are shown in Figs. 4, 5 and 6. Low stability (aggregation state) is shown by the non-functionalized MWCNTs sample when compared with the O-MWCNTs and MgO-MWCNTs. According to ASTM Standard (D 4187–82), moderate stability solvents such as water and ethanol have zeta potential from ±30 to ±40 mV. As the potential value lowers than the standard value, then the attraction surpasses repulsion leading to break down in dispersion and incline to combine. Zeta potential of O-MWCNTs in ethanol decreased from −11 to −16 mV after the acid treatment. The introduction of negatively charged groups on O-MWCNTs could be due to acid treatment (Koch et al. 1999). By the addition of MgO on the surface of MWCNTs, the zeta potential of the hybrid material becomes more positive than the non-

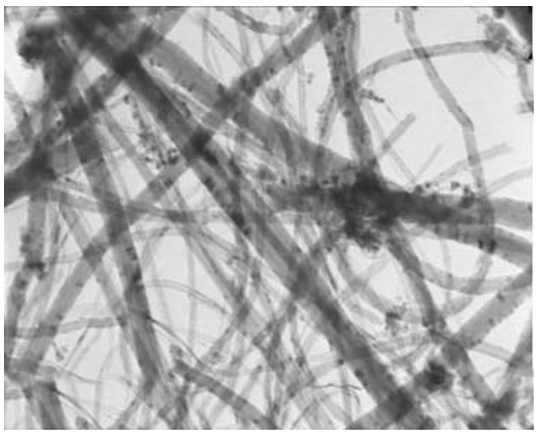

Fig. 9 TEM micrograph of MgO-MWCNTs

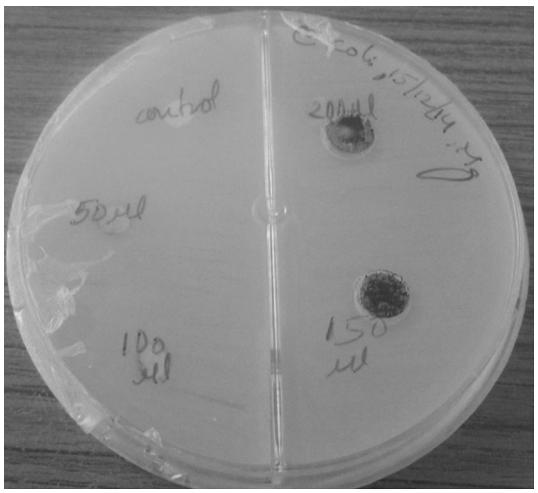

Fig. 10 Inhibition zone test gram-negative bacteria [*E. coli*] for MgO-MWCNTs

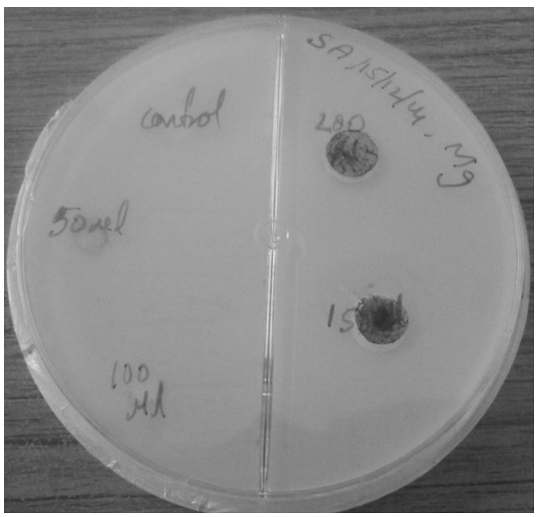

Fig. 11 Inhibition zone test gram-positive bacteria [*S. aureus*] for MgO-MWCNTs

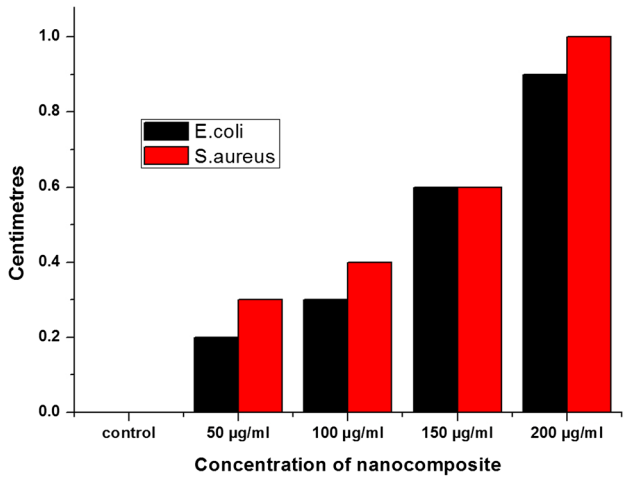

Fig. 12 Graph shows the concentration and zone of inhibition of the *E. coli* and *S. aureus*

functionalized MWCNTs and O-MWCNTs. Therefore, the deposition of metal and metal oxide on the surface of MWCNTs could decrease the original negative charge.

3.5 FE-SEM and TEM

In order to study the surface morphology of the MgO-MWCNTs, FE-SEM characterization has been done. In Figs. 7 and 8 it is observed that nanoparticles exist uniformly and well distributed on the walls of O-MWCNTs. The MgO nanoparticles could be observed. The main advantage of a TEM (Fig. 9) is that it can simultaneously give evidence in real space (in the imaging mode) and reciprocal space (in the diffraction mode).

3.6 Antibacterial test

Due to the advent of nanotechnology, nanomaterials have become an alternative for antibacterial applications. Security, long lasting, no drug resistance and generality are the advantages of nanoantibacterial materials when compared with traditional antibacterial agents (Mohamed Basith et al. 2014). The attention of the researchers has been taken up by the antibacterial activity of CNTs and its composites in the recent times. There are studies in which electrical properties are associated with antibacterial activity (Gonzalez-Campos et al. 2013). Scientists have also discovered that maximum bactericide activity depends on the percolation threshold concentration of the composite. MgO-MWCNTs are tested for antibacterial activity against gram-negative *E. coli* and gram-positive *S. aureus* bacteria. Figs. 10 and 11 show the *E. coli* and *S. aureus* treated with MgO-MWCNTs concentrations ranging from 50 to 200 µg/ml. It is observed that gram-positive bacteria have

more inhibition zone than gram-negative bacteria. Even in the general observation it is well known that positive bacterial strains are more vulnerable than gram-negative strains. This could be explained by the cell wall structure differences (Boudreau et al. 2012). Bacterial inhibition mechanism of nanoparticles is generally related to the production of reactive radicals (Rishnamoorthy and Moon 2012). This mechanism is expected in the study; thus the material's antibacterial activity is related to its capacity in producing such radicals like O^{2-}, –OH and H_2O_2 which might damage the outer membrane wall of bacteria (Amornpitoksuk et al. 2012; Padmavathy and Vijayaraghavan 2008). When MgO-MWCNTs are in direct contact with cell, they could damage the cellular membrane's integrity, surface and metabolic activity of both *E. coli* and *S. aureus*. Thus, the cell membranes of both the bacteria are damaged (Zhu et al. 2010). The antibacterial results are shown in Fig. 12.

4 Conclusion

A facile method for the synthesis of magnesium oxide nanoparticles decorated on O-MWCNTs using magnesium nitrate is described for the first time. The particle size of MgO-MWCNTs is found to be 20–30 nm. The XRD and TEM result confirmed that crystallite size of MgO is 25 nm. The dislocation density and microstrain are 1.65×10^{16} Lines/m^2 and 1.72×10^{-3} Lines^{-2}/m^4, respectively. FT-IR spectra confirm the presence of metal oxygen bond. DTA/TG analysis has showed weight loss is due to vapor, carbon and purity of the composite. The MgO-MWCNTs have exhibited its antibacterial properties on both gram-positive and gram-negative bacterial strains.

References

Amornpitoksuk P, Suwanboon S, Sangkanu S, Sukhoom A, Muensit N, Baltrusaitis J (2012) Synthesis, characterization, photocatalytic and antibacterial activities of Ag-doped ZnO powders modified with a diblock copolymer. Powder Technol 219:158–164

Basavaraja C, Jo EA, Kim BS, Kim DG, Huh DS (2010) Biological templating of polyaniline and polypyrrole using E. coli. Macromol Res 18:222

Boudreau MA, Fisher JF, Mobashery S (2012) Messenger functions of the bacterial cell wall-derived muropeptides. Biochemistry 51(14):2974–2990. doi:10.1021/bi300174x

Campoccia D, Montanaro L, Arciola CR (2013) A review of the biomaterials technologies for infection-resistant surfaces. Biomaterials 34:8533

Carson L, Kelly-Brown C, Stewart M, Oki A, Regisford G, Luo Z, Bakhmutov VI (2009) Synthesis and characterization of chitosan–carbon nanotube composites. Mat Lett 63:617

Chung KT, Chen SC, Wong TY, Wei CI (1998) Effects of benzidine and benzidine analogues on growth of bacteria including Azotobacter vinelandii. Environ Toxicol Chem 17:271–275

DeJesus JC, González I, Quevedo A, Puerta T (2005) Thermal decomposition of nickel acetate tetrahydrate: an integrated study by TGA, QMS and XPS techniques. J Mol Catal A 228:283

Erdema A, Mutia M, Karadeniza H, Congura G, Canavara E (2012) Electrochemical monitoring of indicator-free DNA hybridization by carbon nanotubes–chitosan modified disposable graphite sensors. Colloid Surf B Biointer 95:222

Gonzalez-Campos JB, Mota-Morales JD, Kumar S, Zarate-Trivino D, Hernandez-Iturriaga M, Prokhorov E, Vazquez-Lepe M, Garcıa-Carvajal ZY, Sanchez IC, Luna-Barcenas G (2013) New insights into the bactericidal activity of chitosan-Ag bionanocomposite: the role of the electrical conductivity. Colloid Surf B Biointer 111:741

Hao C, Ding L, Zhang X, Ju H (2007) Biocompatible conductive architecture of carbon nanofiber-doped chitosan prepared with controllable electrodeposition for cytosensing. Anal Chem 79:4442

Ke G, Guan W, Tang C, Guan W, Zeng D, Deng F (2007) Covalent functionalization of multiwalled carbon nanotubes with a low molecular weight chitosan. Biomacromolecules 8:322

Khare R, Bose S (2005) Carbon nanotube based composites-a review. J Min Mater Character Eng 41:31–46

Koch S, Woias P, Meixner LK, Drost S, Wolf H (1999) Protein detection with a novel ISFET-based zeta potential analyzer. Biosens Bioelectron 14:417–425

Kondoh K, Fukuda H, Umeda J, Imai H, Fugetsu B, Endo M (2010) Microstructural and mechanical analysis of carbon nanotube reinforced magnesium alloy powder composites. Mater Sci Eng A 527:4103–4108

Lin KY, Tsai WT, Chang JK (2010) Decorating carbon nanotubes with Ni particles using an electroless deposition technique for hydrogen storage applications. J Int, Hydrog Energy 35:7555

Liu F, Zhang XB, Haussler D, Jager W, Yi GF, Cheng JP, Tao XY, Luo ZQ, Zhou SM (2006) TEM characterization of metal and metal oxide particles supported by multi-wall carbon nanotubes. J Mater Sci 41:4523

Liu YL, Chen WH, Chang YH (2009) Preparation and properties of chitosan/carbon nanotube nanocomposites using poly(styrene sulfonic acid)-modified CNTs. Carbohydr Polym 76:232

Makhluf S, Dror R, Nitzan Y, Yaniv A, Jelenik R, Gedanken A (2005) Microwave-assisted synthesis of nanocrystalline MgO and its use as a bacteriocide. Adv Funct Mater 15:1708–1715

Mohamed Basith N, Judith Vijaya J, John Kennedy L, Bououdina M, Jenefar S, Kaviyarasan V (2014) Co-doped ZnO nanoparticles: structural, morphological, optical, magnetic and antibacterial studies. J Mater Sci Technol 30(11):1108–1117

Nagappa B, Chandrappa GT (2007) Mesoporous nanocrystalline magnesium oxide for environmental remediation. Microporous Mesoporous Mater 106:212–218

Padmavathy N, Vijayaraghavan R (2008) Enhanced bioactivity of ZnO nanoparticles—an antimicrobial study. Sci Technol Adv Mater 9:035004

Pal J, Chauhan P (2009) Structural and optical characterization of tin dioxide nanoparticles prepared by a surfactant mediated method. Mater Charact 60:1512

Park C, Ounaies Z, Watson KA, Pawlowski K, Lowther SE, Connell JW, Siochi EJ, Harrison JS, St. Clair TL (2002) Polymer-single wall carbon nanotube composites for potential spacecraft applications. Nasa Langley Research Center

Pauliukaite R, Ghica ME, Fatibello-Filho O, Brett CMA (2010) Electrochemical impedance studies of chitosan-modified electrodes for application in electrochemical sensors and biosensors. Electrochim Acta 55:6239

Rishnamoorthy K, Moon JY, Hyun HB, Cho SK, Kim S-J (2012) Mechanistic investigation on the toxicity of MgO nanoparticles toward cancer cells. J Mater Chem 22(47):24610–24617

Sahoo S, Husale S, Karna S (2011) Controlled assembly of Ag nanoparticles and carbon nanotube hybrid structures for biosensing. J Am Chem Soc 133(11):4005–4009

Sawai J (2003) Quantitative evaluation of antibacterial activities of metallic oxide powders (ZnO, MgO and CaO) by conductimetric assay. J Microbiol Methods 54(2):177–182

Sawai J, Kojima H, Igarashi H, Hashimoto A, Shoji S, Sawaki T, Hakoda A, Kawada E, Kokugan T, Shimizu M (2000) Antibacterial characteristics of magnesium oxide powder. World J Microbiol Biotech 16(2):187–194

Shameli K, Ahmad MB, Al-Mulla EAJ (2012) Green biosynthesis of silver nanoparticles using Callicarpa maingayi stem bark extraction. Molecules 17(7):8506–8517

Shameli K, Ahmad MB, Al-Mulla EAJ, Shabanzadeh P, Bagheri S (2013) Antibacterial effect of silver nanoparticles on talc composites. Res Chem Intermed. doi:10.1007/s11164-013-1188-y

Shieh YT, Yang YF (2006) Significant improvements in mechanical property and water stability of chitosan by carbon nanotubes. Eur Polym J 42:3162

Stoimenov PK, Klinger RL, Marchin GL, Klabunde KJ (2002) Metal oxide nanoparticles as bactericidal agents. Langmuir 18:6679

Tang C, Chen N, Zhang Q, Wang K, Fu Q, Zhang X (2009) Preparation and properties of chitosan nanocomposites with nanofillers of different dimensions. Polym Degr Stab 94:124

Titus E, Ali N, Cabral G, Gracio J, Babu PR, Jackson MJ (2006) Chemically functionalized carbon nanotubes and their characterization using thermogravimetric analysis, fourier transform infrared, and raman spectroscopy. J Mater Eng Perform 15:182

Tiwari DK, Behari J, Sen P (2008) Application of nanoparticles in waste water treatment. World App Sci J 3(3):417–433

Wang SF, Shen L, Zhang WD, Tong YJ (2005) Preparation and mechanical properties of chitosan/carbon nanotubes composites. Biomacromolecules 6:3067

Xu C, Wu G, Liu Z, Wu D, Meek TT, Han Q (2004) Preparation of copper nanoparticles on carbon nanotubes by electroless plating method. Mater Res Bulletin 39:1499–1505

Zhu X, Bai R, Wee KH, Liu C, Tang SL (2010) Membrane surfaces immobilized with ionic or reduced silver and their antibiofouling performances. J Membr Sci 363:278